Concentration Effect on the Absorption and Emission Spectra of the 9-Oxa-2,3,4′-methoxybenzobicyclo[4.3.0]non-1(6)-ene-7,8-dione: Self-Associated Dimer and Excimer

M. Dkaki, S. Ait-Lyazidi,* and M. Haddad

Laboratoire de Spectronomie Physique, Université My Ismaïl, Faculté des Sciences, B.P 4010 Beni M'hamed, Meknès, Morocco

M. Hnach

Département de Chimie, Faculté des Sciences et Techniques Errachidia, Errachidia, Morocco

C. Cazeau-Dubroca

Centre de Physique Moléculaire Optique et Hertzienne, UA 283 CNRS, Université Bordeaux I, 351 Cours de la Libération, Talence 33405, France

J. P. Aycard

Laboratoire de Physique des Interactions Ioniques et Moléculaires, URA 773, Université de Provence, 13397 Marseille, Cedex 20, France

Received: January 9, 1997; In Final Form: November 4, 1997

Ground and excited state self associations are observed in solution at room temperature in the case of the 9-oxa-2,3,4′-methoxybenzobicyclo[4.3.0]non-1(6)-ene-7,8-dione molecule. Depending on the solute concentration, the ground state associated forms are attributed to a dimer involving interaction between only two solute molecules, or to an aggregate of higher order. The theoretical simulation, using the analytical atom−atom pair potential described below, predicts several energy minima of the dimer. The two most stable dimer's structures are those involving a face-to-face slipped structure with head-to-tail orientation. An excimer emission is also observed subsequently to the excitation by either the absorption monomer bands or by the absorption band of the van der Waals dimer. The two adjacent molecules forming the excimer species are readily in approximately parallel planes.

1. Introduction

Furan-2,3-dione derivatives have been widely studied because of their biological activity as carcinostatic compounds.[1] The studies of the reactivity of these compounds via photolysis experiments involve a good knowledge of their absorption and emission spectra. In order to interpret correctly the electronic transitions in the absorption spectrum of the 9-oxa-2,3,4′-methoxybenzobicyclo[4.3.0]non-1(6)-ene-7,8-dione: $C_{13}H_{10}O_4$ (compound **A**), we have studied, in a previous work,[2] the UV−vis absorption linear dichroism (LD) spectra of this compound aligned in uniaxially stretched polyethylene (PE) film. Such measurements have provided experimental information on the number, position, and polarization of the electronic transitions. Nevertheless, because of its high permanent dipole moment (8.6 D), this compound can give rise to self associated forms in solutions at room temperature.

In this work, at first, we have been interested in the concentration effect on the absorption spectrum from 10^{-6} to 10^{-2} M, as well as a simulation of the ground state dimer using the improved analytical Fraga's atom−atom pair potential (FAAP) described below.

Continuing the research on the self-association process of the compound **A** in solutions at room temperature, we have also studied the concentration effect on the stationary fluorescence and excitation spectra of this compound. We attempted thus to detect excited dimeric species (i.e., excited van der Waals (vdw) dimers or excimers).

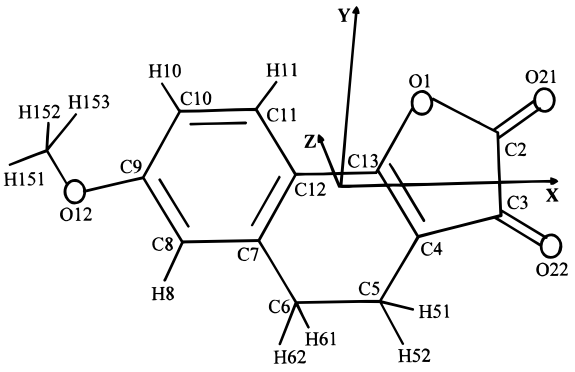

Compound A

2. Experimental Section

The synthesis of this compound has been reported elsewhere.[3] The solvents used are of spectroscopic quality. The UV−vis absorption spectra were recorded on a Shimadzu model UV-

S1089-5639(97)00151-5 CCC: $15.00
Published on Web 06/17/1998

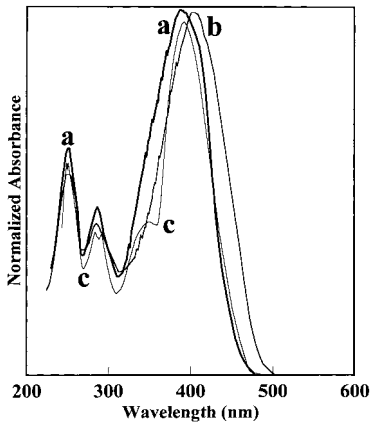

Figure 1. Room temperature absorption spectra of compound **A** at 10^{-6} M: (a) in chloroform, (b) in acetonitrile, and (c) aligned in stretched PE film.

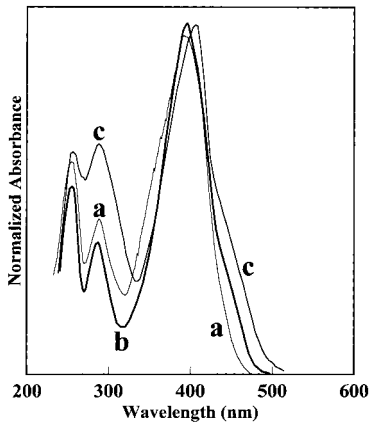

Figure 2. Room temperature absorption spectra of compound **A** at (a) 5×10^{-6} M in chloroform, (b) 5×10^{-5} M in chloroform, and (c) 5×10^{-5} M in acetonitrile.

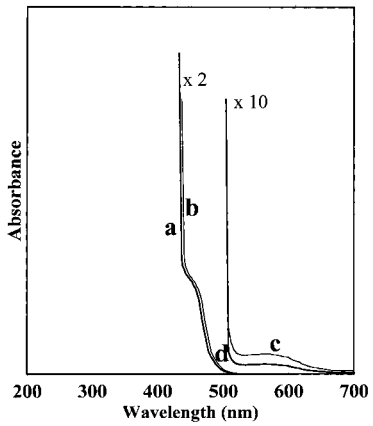

Figure 3. Room temperature absorption spectra of compound **A** at (a) 5×10^{-4} M in chloroform, (b) 5×10^{-4} M in acetonitrile, (c) 10^{-2} M in chloroform, and (d) 10^{-2} M in acetonitrile.

2100 spectrometer; the stationary fluorescence and excitation spectra were measured on a PERKIN ELMER MPF-2A spectrofluorimeter.

3. Results and Discussion

3.1. Room Temperature UV−Vis Absorption Spectra at low Concentration. In Figure 1a and 1b are reported the room temperature absorption spectra of the 9-oxa-2,3,4′-methoxybenzobicyclo[4.3.0]non-1(6)-ene-7,8-dione molecule, called compound **A**, in chloroform and acetonitrile at the concentration $C = 10^{-6}$ M. The spectrum, in both solvents, presents three main bands. The highest energy bands are located respectively around $\lambda_{max} = 256$ nm and $\lambda_{max} = 290$ nm; the lowest energy band, broad and more intense, is situated around $\lambda_{max} = 396$ nm. This band is red shifted of about 12 nm when the solvent polarity is increased from chloroform ($\epsilon = 4.7$) to acetonitrile ($\epsilon = 37.5$), while the formers remain unchanged. In the last work,[2] we have investigated UV−vis linear dichroism spectra of the compound **A** aligned in stretched polyethylene (PE) film as well as CNDO/S calculations. The UV−vis LD spectrum was resolved into four electronic transitions differently polarized (Figure 1c). The first transition at $\lambda_{max} = 396$ nm is polarized along the long axis of the molecule. This band which presents some intramolecular charge-transfer character corresponds to the $\pi\pi^*$ transition of the $C_3{=}O_{22}$ carbonyl chromophore. The second transition at $\lambda_{max} = 360$ nm, which is hidden by the first one in solution, is clearly isolated in the LD absorption spectrum (Figure 1c) and is polarized along some intermediate direction between the long and the in-plane short axis of the molecule. This transition is attributed to the $\pi\pi^*$ one of the $C_2{=}O_{21}$ carbonyl chromophore. The third transition at $\lambda_{max} = 290$ nm and the fourth one at $\lambda_{max} = 256$ nm are polarized perpendicularly each to other. They correspond respectively, to the ^1L_b and ^1L_a transitions of the benzene part in the molecule.[2]

3.2. Room Temperature UV−Vis Absorption at High Concentration. Figures 2 and 3 show the variation of the absorption spectrum of the compound **A**, in chloroform and acetonitrile, with increasing the concentration from 5.10^{-6} to 10^{-2} M. At the lower concentration the spectrum corresponds to that of the monomer described above in Figure 1. When the concentration is about 5.10^{-5} M, the spectrum undergoes a net red edge broadening around 460 nm (Figure 2b and 2c). As the concentration of the compound **A** is increased until 5.10^{-3} M, the room temperature absorption spectrum, in both chloroform and acetonitrile, shows a new band at 460 nm (Figures 3a and 3b). The relative intensity of this new red edge band, compared to that of the first monomer $\pi\pi^*$ transition located at 396 nm, is very weak. This weakness does not permit to observe simultaneously the new band and the other $\pi\pi^*$ bands of the monomer. We have attributed this new red edge absorption band, at 460 nm, to the formation of a self-associated dimer of the compound **A**. The dimer is the first self-associated form which can appear at the ground state without perturbing much the absorption spectrum of the monomer. Numerous experimental and theoretical studies of such systems have been published.[4−9] Otherwise, contrary to the lowest energy band of the monomer, the dimer band, which is located at 460 nm, remains unchanged when the solvent polarity is increased (Figures 3a and 3b). This is indicative that the self-dimer of the compound **A** has a dipole moment inferior to that of the monomer.[10]

At higher concentration, $C \approx 10^{-2}$ M, the spectrum reveals a new band around 580 nm (Figures 3c and 3d). This new band has an intensity so weak that it is impossible to observe it all together with those of the monomer and the dimer. Similarly to the dimer band, this new broad band located between 520 and 620 nm, is independent on the solvent polarity; this new feature is most probably du to the formation of a ground state higher order complex, larger than the dimer and consisting in the interaction of three or more solute molecules. Clusters were also observed at room temperature in the case of naphthalene.[11−13]

3.3. Theoretical Modeling of the Self Dimer Association. *Method.* To modelize the self associated dimer of the compound

A, we have used the analytical atom−atom pair potential proposed previously by Fraga (FAAP)[14−18] and improved by Sanchez-Marin et al.[19−21] In this pairwise potential, the interaction energy ΔE between two molecules *A* and *B*, assumed to be rigid sets of individual atoms, is obtained as summation of atom *i* (of *A*) to atom *j* (of *B*) contributions (ΔE_{ij}) which have the form of an expansion in powers of $1/R_{ij}$ such as

$$\Delta E = \sum_{i}^{A}\sum_{j}^{B}\Delta E_{ij} \quad (1)$$

with

$$\Delta E_{ij}^{ab} = 1389.4168\, q_i^a\, q_j^b/R_{ij} - 694.70838\,(f_i^a\,\alpha_i^a(q_j^b)^2 + f_j^b\,\alpha_j^b(q_i^a)^2)/R_{ij}^4 - 1516.0732\, f_i^a\,\alpha_i^a\, f_j^b\,\alpha_j^b/\{(f_i^a\,\alpha_i^a/n_i^a)^{1/2} + (f_j^b\,\alpha_j^b/n_j^b)^{1/2}\}R_{ij}^6 + 4.184\, c_i^a\, c_j^b/R_{ij}^{12} \quad (2)$$

where *q* is the net atomic charge, α is the isotropic polarizability, $n = Z - q$ is the effective number of electrons, and *f* and *c* are parameters that were adjusted to reproduce Clementi's potentials.[22−24] The superscripts a and b denote the classes to which belong the atoms *i* and *j* respectively, taking into account their environments in the respective molecule. Parameters (*q*, α, *f*, *c*) for H, Li, C, N, O, Na, S, K, and Ca can be assigned to 82 classes reported in refs 15−18. R_{ij} is the separation between the two interacting atoms *i* and *j*. The interaction energy is given in kJ mol^{-1} when α is in Å^3, *c* is in Kcal$^{1/2}$ Å^6 mol$^{-1/2}$, and R_{ij} is in angstroms.

To improve the behavior of the potential at short distances, an empirical correction E_{ij}^D of the dispersion energy term is included by using a new R^{-6} term that is added to the original potential like a second R^{-6} term.[19,25]

$$E_{ij}^D = -1516.0732\,\alpha_i^a\,\alpha_j^b/\{(\alpha_i^a/n_i^a)^{1/2} + (\alpha_j^b/n_j^b)^{1/2}\}R_{ij}^6 \quad (3)$$

This additional term has the same form and parameters of the original R^{-6} one, but the scaling factor *f* are now set to one. The total pair potential incorporating the new correction is then:

$$\Delta E_{tot} = \sum_{i}^{A}\sum_{j}^{B}\Delta E_{ij} + \sum_{i}^{A}\sum_{j}^{B}E_{ij}^D \quad (4)$$

The version, of the program, used in this work is that adopted by Torrens and co-workers.[25] The program allows for the determination of stable conformations of the association of two molecules. These conformations are found by minimization of the interaction energy between the two molecules *A* and *B*. Both systems are kept rigid throughout the energy minimization process. The center of mass of molecule *A* is always held in the origin of the coordinates, and the orientation of this molecule is kept fixed in the space. The position of the molecule *B* is expressed, in each new step of the optimization process, by means of a 6-fold vector $R = (x, y, z, \alpha, \beta, \gamma)$. The three first values indicate translations along the cartesian axis *X*, *Y*, and *Z*; the three second values show successive rotations around these axis, respectively. The crystallographic structure of the studied molecule was reported by Bonnaud and Hnach.[26] Furthermore, the atomic charges and the dipole moment μ, used in this calculation, are those obtained directly from other previous ab initio calculations.

Calculation Results. Table 1 collects the total interaction energy as well as the geometric parameters of the two most stable conformations of the dimer. Reported in Figure 4 are the geometrical structures corresponding to the stacked dimers. These arrangements of the homo-dimer are face-to-face slipped structures with head-to-tail mutual orientation. Thus the preferred configuration of the present dimer is the two displaced parallel molecules with their dipole moments opposed. The opposing dipole moments lead to stabilization of the dimer by dipole−dipole interactions. A similar geometry was reported by Lim[27] in the case of dibenzofuran dimer and by Torrens[20] in the case of some azine dimers. These face-to-face rotated structures lead to a dipole moment for the dimer of about 5.9 D for minimum **D$_1$** and 8 D for minimum **D$_2$** (i.e., lower than that of the monomer A which is of about 8.6 D). The two stacked structures are important for the geometrical description of the most stable arrangement of the two interacting molecules. As shown in Figure 4 and in Table 1, the plane of the benzene part in each molecule is exactly parallel to that one in the other molecule. The equilibrium distances between the centers of the two benzene parts are 3.32 Å for minimum **D$_1$** and 3.58 Å for minimum **D$_2$**. These values agree with that reported by Torrens et al.[19] for the face-to-face benzene−benzene dimer (i.e., 3.8 Å) and close to the interplanar separation 3.4−3.6 Å between two interacting porphyrins as reported by Hinter et al.[28]

TABLE 1: Calculated Interaction Energies, Dipole Moments, and Geometrical Parameters for the two Most Stable Dimer Structures D$_1$and D$_2$

minimum	E_{tot}[a]	d[b]	α[c]	β[c]	γ[c]	μ[d]	Φ[e]	z[e]
D$_1$	−710.78	5.07	180.0	180.0	−128.0	5.9	176.0	3.32
D$_2$	−690.67	7.60	−238.0	−208.0	105.0	8.0	178.0	3.58

[a] The total interaction energy (in kJ/mol). [b] Distance between the centers of mass of the two interacting molecules (in angstroms). [c] Rotation angles around the *X*, *Y*, and *Z* axis, respectively, (in degrees). [d] Calculated dipole moment (in debyes). [e] Φ (angle, in degrees) and *z* (separation, in angstroms) between the planes of the two benzene parts.

The great difference between the dimers **D$_1$** and **D$_2$** consists in the fact that their dipole moments are respectively 5.9 and 8 D. The observed non dependence of the dimer band on solvent polarity (Figures 3a and 3b) seems to indicate that the geometrical structure **D$_1$** is the most probable dimer configuration. Nevertheless the relatively high dipole moments values obtained for these dimers may be related to an eventual uncertainty of the theoretical FAAP calculation. Furthermore, the calculated interatomic distances, $O_1^{(A)}\,C_{10}^{(B)} = 3.670$ Å and $O_1^{(A)}\,H_{10}^{(B)} = 3.040$ Å, between the two interacting molecules in the dimer **D$_1$** are very close to those reported for a pair of neighboring molecules in the crystal[26] (i.e., 3.677 and 3.060 Å, respectively).

3.4. UV−Vis Fluorescence and Excitation Spectra: Concentration Effect. Figure 5 presents the concentration dependence of the fluorescence spectrum of the compound **A** from 5×10^{-6} to 10^{-3} M, in chloroform, when the sample is excited by the monomer absorption band around 300 nm. The fluorescence spectrum of the more diluted solution (i.e., $C = 5 \times 10^{-6}$ M) corresponds to the normal fluorescence of the monomeric species (Figure 5a). As the solute concentration is increased, a new emission band appears around 520 nm (i.e., at the lower energy side of the normal fluorescence spectrum). Its intensity increases with increasing the concentration, and it remains unchanged when the solvent polarity is varied from chloroform to acetonitrile in which we have observed the same behavior.[29] Since the sample was excited by the monomer absorption band located around 300 nm, the observed anomalous emission at 520 nm (Figure 5) is characteristic of excimer formation. In our previous work,[29] we have found the excimer-

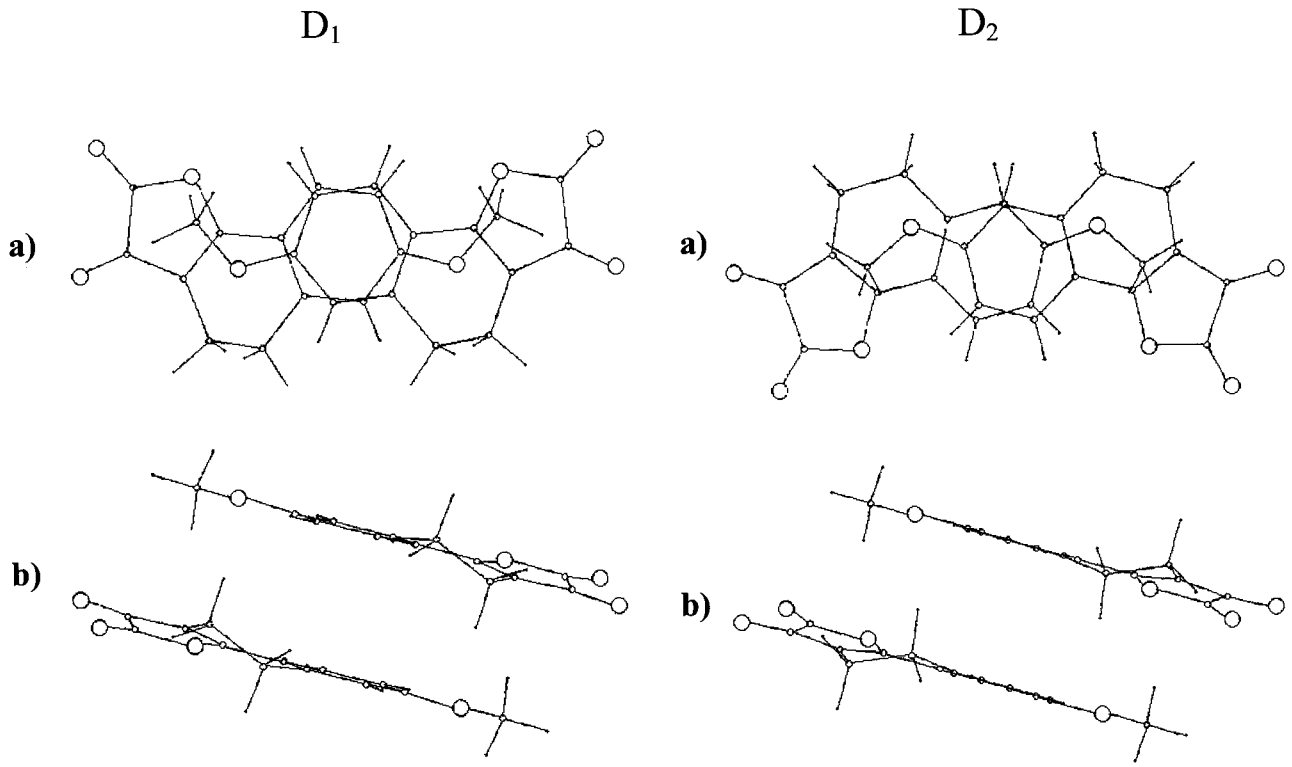

Figure 4. Structures of the two stable dimer minima $\mathbf{D_1}$ and $\mathbf{D_2}$ viewed (a) from the axis perpendicular to the molecular plane and (b) from the short in-plane molecular axis.

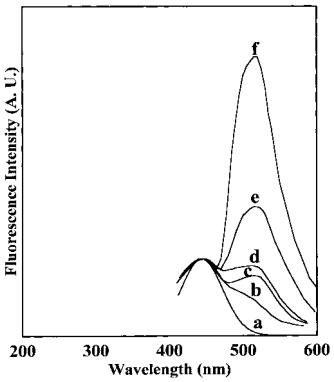

Figure 5. Room temperature fluorescence spectra of the compound **A** in chloroform at different concentrations (excitation at 300 nm). (a) 5×10^{-6} M, (b) 5×10^{-5} M, (c) 10^{-4} M, (d) 2.5×10^{-4} M, (e) 5×10^{-4} M, and (f) 10^{-3} M. The spectra are normalized at the monomer emission peak at 445 nm.

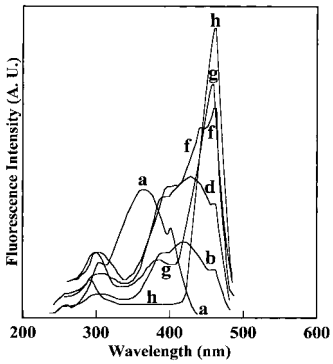

Figure 6. Room temperature excitation spectra of the compound **A** in chloroform at different concentrations (emission at 520 nm). (a) 5×10^{-6} M, (b) 5×10^{-5} M, (d) 2.5×10^{-4} M, (f) 10^{-3} M, (g) 2.5×10^{-3} M, and (h) 5×10^{-3} M.

to-monomer emission intensity ratio, as generally expected,[30] to increase linearly with increasing solute concentration in both chloroform and acetonitrile, and to be more important as the solvent viscosity is decreased from $\eta = 542$ cp (in chloroform) to $\eta = 345$ cp (in acetonitrile).

Since the absorption spectrum is also dependent on the solute concentration (Figure 2 and 3), we have measured in parallel with the emission curves the corresponding excitation spectra (Figure 6), at $\lambda_{em} = 520$ nm, in the concentration range of 5×10^{-6} to 5×10^{-3} M. The major observation that can be made consists in the large dependence of the excitation spectrum on the solute concentration. For the more diluted solution ($C = 5 \times 10^{-6}$ M) the excitation spectrum (Figure 6a) corresponds to that of the normal fluorescence. It shows all the spectral features observed in the monomer absorption spectrum, located respectively around 256, 290, 360, and 396 nm. As the concentration is increased, the above excitation spectrum changes similarly to the absorption spectrum (Figure 2 and 3) of the studied compound. At first this excitation spectrum, monitored at $\lambda_{em} = 520$ nm, shows a large red edge broadening (Figure 6b). When the concentration is about $C = 10^{-3}$ M, a new band appears distinctly at 460 nm with a high efficiency (Figure 6f). At concentrations above 10^{-3} M (Figure 6h) all the monomer bands, located between 256 and 400 nm, are highly quenched to the profit of the new band at 460 nm, which corresponds to the absorption band of the ground-state vdw dimer of the compound **A**. Hence, we can conclude that the new band observed at 520 nm in the emission spectrum is subsequent to excitation by either the absorption monomer bands, located between 250 and 400 nm, or by the dimer absorption band situated at 460 nm. Therefore, it may be concluded that this long wavelength emission band, around 520 nm, can originate either from the excited vdw dimer or from a product of photoassociation (i.e., an excimer). The excited states of such molecular clusters are classified as an electronically excited vdw dimer or an excimer depending on whether the ground electronic

state is attractive or repulsive for the molecular configurations corresponding to the excited species.[31,32]

Since the emission spectrum shows exactly the same long wavelength emission band at 520 nm following the excitation of the monomer or the ground state vdw dimer, leading respectively to the excimer or to the excited dimer species, we have made the hypothesis that one of these two excited clusters is readily convertible to the other during the lifetime of the emitting state.[29]

Other reported works[33−37] underlined that excited vdw dimers having two adjacent molecules in approximately parallel planes, as it is the case, undergo relaxation into excimer states. This implies a large coupling between the excited vdw dimer and the excimer states.[29]

4. Conclusion

Room temperature self associations of the 9-oxa-2,3,4′-methoxybenzobicyclo[4.3.0]non-1(6)-ene-7,8-dione molecule are observed in solution depending on the solute concentration. The first red edge absorption band which appears around 460 nm, at a concentration about 5×10^{-5} M, is attributed to the formation of dimeric forms involving interactions between two solute molecules. The second band, which appears around 580 nm, at higher concentration (i.e., $C \approx 10^{-2}$ M) is assigned to the apparition of an aggregate, of higher order, involving the association of three or more solute molecules. These bands remain unchanged when the solvent polarity is increased from chloroform to acetonitrile.

The investigated theoretical simulation of the dimer form, using the improved Fraga's atom−atom pair potential (FAAP), suggests that the most stable geometrical structure of the homodimer is the face-to-face with head-to-tail slipped one.

In parallel with the absorption spectra, we have also investigated the study of the room-temperature emission and excitation spectra in the concentration range 5×10^{-6} to 5×10^{-3} M. At sufficiently high concentrations, on top of the monomer fluorescence band, an excimer emission band appears subsequently to the excitation by either the monomer absorption bands or by the absorption band of the ground state dimer. This seems to involve a large coupling between the excited vdw dimer and the excimer states.

In the near future we plane to undertake (i) CNDO/S calculations in order to estimate theoretically the location and the oscillator strength of the first absorption band of the two possible dimers $\mathbf{D_1}$ and $\mathbf{D_2}$, (ii) the study of the temperature effect on the formation of the self-associated dimer, aggregate, and excimer of the present Furane 2,3-dione derivative.

Acknowledgment. We are grateful to Professor L. Fernandez Pacios, from the Universidad Politecnica de Madrid, who kindly permitted us to have the improved version of Fraga's program. Also, we thank Professor J. Sanchez-Marin, from the Universitat de Valencia, for his fruitful discussions.

References and Notes

(1) Douglas, K. T.; Shinkai, S. *Angew. Chem., Int. Ed. Engl*. **1985**, *2*, 31.
(2) Ait-Lyazidi, S.; Dkaki, M.; Hnach, M.; Aycard, J. P.; Cazeau-Dubroca, C. *Spectrochim. Acta A* **1997**, *53*, 605.
(3) Hnach, M.; Aycard, J. P.; Zineddine, H. *Bull. Soc. Chim. Fr*. **1991**, *128*, 393.
(4) Rabinowitch, E.; Epstein, L. F. *J. Am. Chem. Soc*. **1941**, *63*, 69.
(5) Ameloot, M.; Boens, N.; Andriessen, R.; Van Den Bergh, V.; De Schryver, F. C. *J. Phys. Chem.* **1991**, *95*, 2041.
(6) Andriessen, R.; Boens, N.; Ameloot, M.; De Schryver, F. C. *J. Phys. Chem.* **1991**, *95*, 2047.
(7) Declercq, D.; Delbeke, P.; De Schryver, F. C.; Van Meervelt, L.; Miller, R. D. *J. Am. Chem. Soc*. **1993**, *115*, 5702.
(8) Burdett, B. C. *Aggregation Processes in Solution*; Jones, E. W., Gormally, J., Eds.; Elsevier: Amsterdam, 1983.
(9) Valdes Aguilera, O.; Neckers, D. C. *Acc. Chem. Res* **1989**, *22*, 171.
(10) Foster, R. *Molecular Association*; Academic Press: London, 1975.
(11) Saigusa, H.; Sun, S.; Lim, E. C. *J. Phys. Chem.* **1992**, *96*, 2083.
(12) Saigusa, H.; Sun, S.; Lim, E. C. *J. Phys. Chem.* **1992**, *96*, 10099.
(13) Saigusa, H.; Sun, S.; Lim, E. C. *J. Phys. Chem.* **1992**, *97*, 9072.
(14) Fraga, S.; Saxena, K. M. S.; Torres, M. *Biomolecular Information Theory, Studies in Physical and Theoretical Chemistry*; Elsevier: Amsterdam, 1978.
(15) Fraga, S. J. *Comput. Chem*. **1982**, *3*, 329.
(16) Fraga, S. *Comput. Phys. Commun*. **1983**, *29*, 351.
(17) Nilar, S. H. M.; Fraga, S. *J. Comput. Chem*. **1984**, *5*, 261.
(18) Sordo, J. A.; Fraga, S. *J. Comput. Chem*. **1986**, *7*, 55.
(19) Torrens, F.; Sanchez-Marin, J.; Orti, E.; Nebot-Gil, I. *J. Chem. Soc., Perkin Trans*. **1987**, *2*, 943.
(20) Torrens, F.; Sanchez de Meras, A. M.; Sanchez-Marin, J. *J. Mol. Struct. (THEOCHEM)* **1988**, *166*, 135.
(21) Torrens, F.; Sanchez-Marin, J.; Tomas, F. *J. Chem. Res*. **1990**, 176.
(22) Clementi, E. *Computational Aspects for Large Chemical Systems, Lecture Notes in Chemistry*; Springer-Verlag: Berlin, 1980.
(23) Clementi, E.; Cavallone, F.; Scordamaglia, R. *J. Am. Chem. Soc.* **1977**, *99*, 5531.
(24) Scordamaglia, R.; Cavallone, F.; Clementi, E. *J. Am. Chem. Soc.* **1977**, *99*, 5545.
(25) Torrens, F.; Orti, E.; Sanchez-Marin, *J. Comput. Phys. Commun*. **1991**, *66*, 341.
(26) Bonnaud, B.; Hnach, M.; Aycard, J. P.; Lapasset, J. *J. Cryst. Spectrosc. Res*. **1993**, *23*, 563.
(27) Chakraborty, T.; Lim, E. C. *Chem. Phys. Lett*. **1993**, *207*, 99.
(28) Hunter, C. A.; Sanders, J. K. M. *J. Am. Chem. Soc.* **1990**, *112*, 5525.
(29) Cazeau-Dubroca, C.; Dkaki, M.; Ait-Lyazidi, S.; Sbai, M.; Hnach, M.; Aycard, J. P. *Recent Research Developments in Photochemistry & Photobiology*; Transworld Research Network: New York. In press.
(30) Birks, J. B. *Photophysics of Aromatic Molecules*; Wiley-Interscience: New York, 1970.
(31) Mataga, N.; Kubota, T. *Molecular Interaction and Electronic Spectra*; Marcel Dekker, Inc.: New York, 1970.
(32) Modiano, S. H.; Dresner, J.; Lim, E. C. *Chem. Phys. Lett*. **1992**, *189*, 144.
(33) Chakraborty, T.; Lim, E. C. *Chem. Phys. Lett*. **1993**, *207*, 99.
(34) Saigusa, H.; Lim, E. C. *J. Phys. Chem.* **1995**, *99*, 15738.
(35) Wessel, J. E.; Sayage, J. A. *J. Phys. Chem.* **1988**, *89*, 5962.
(36) Wessel, J. E.; Sayage, J. A. *J. Phys. Chem.* **1990**, *94*, 737.
(37) Saigusa, H.; Itoh, M. *J. Phys. Chem.* **1985**, *89*, 5436.